JOURNAL OF GEOPHYSICAL RESEARCH, VOL. 104, NO. A5, PAGES 10,041–10,049, MAY 1, 1999

Electron energy balance in the F region above Jicamarca

Nestor Aponte,[1] Wesley E. Swartz, and Donald T. Farley
School of Electrical Engineering, Cornell University, Ithaca, New York

Abstract. Incoherent scatter measurements from Jicamarca, Peru, show that current models and cross sections account quite well for the heating and cooling of F region electrons, in marked contrast to earlier similar studies at low and middle latitudes. The latter showed discrepancies of the order of a factor of 2 between the calculated energy input and loss rates. The equatorial F region ionosphere provides the simplest configuration for such studies because the horizontal magnetic field eliminates vertical photoelectron transport and thermal conduction. We based our estimates of electron heating on photoelectron energy spectra computed from recently developed solar flux models and new absorption and ionization cross sections and included the additional energy source due to quenching of the ^2D metastable state of nitrogen. This extra source is sometimes significant. Electron and ion temperatures and densities measured with the Jicamarca incoherent scatter radar were used to complete the calculations of the heating and cooling rates. We present here data from 2 days, one with low solar activity and one with moderate activity, over the altitude range 220–325 km. The heating/cooling rates ranged from about 500 to 6000 eV cm^{-3} s^{-1}. Over this entire range the calculated heating and cooling rates differed by 10% or less when the data quality was good.

1. Introduction

Modelers of the Earth's ionosphere and plasmasphere [e.g., *Bailey and Sellek*, 1990; *Richards and Torr*, 1988] solve a set of energy balance equations to estimate the temperatures of the ions and electrons. Although the basic processes responsible for the electron energy balance in the F region are well understood [*Schunk and Nagy*, 1978], early studies designed to test quantitatively this energy balance in the F region at middle and low latitudes found discrepancies of the order of a factor of 2 between the heating and cooling rates [e.g., *Swartz and Nisbet*, 1973; *Pingree*, 1990]. Such differences imply errors of several hundred degrees in any model calculations that used the same rates.

These and other studies of the electron energy balance in the F region during the 1970s and 1980s lacked accurate estimates of a key parameter, the solar EUV flux. Measurements of this parameter are still scarce. During the last decade or so, however, several proxies to the EUV flux were introduced [e.g., *Tobiska and Barth*, 1990; *Tobiska*, 1991; *Richards et al.*, 1994; *Tobiska and Eparvier*, 1998]. Recently, *Richards and Khazanov* [1997] looked at the thermal balance at middle latitudes using incoherent scatter data from Millstone Hill and the updated EUV proxies. They found that they still needed to double the heating of the plasmasphere (by photoelectrons escaping from both conjugate ionospheres) to reproduce the observed topside temperatures; that is, the calculated cooling rates greatly exceeded the solar heating.

We felt it was worthwhile to have another look at this problem using equatorial data, since there, the horizontal magnetic field eliminates the twin complications of (1) nonlocal photoelectron heating (by electrons created at altitudes possibly far from the altitude of the measurement) and (2) vertical thermal conduction. As a result, we can simplify the general electron energy balance equation of *Schunk and Nagy* [1978] to a purely local form. In the remainder of this paper we show that, at least at the equator, the most recent models of the various heating and cooling processes do, in fact, account very nicely for the observed (by incoherent scatter) temperature variations in the F region.

2. Electron Heating and Cooling

At low and middle latitudes the ambient electron gas is heated primarily through Coulomb collisions with energetic photoelectrons that are created by solar EUV [e.g., *Swartz and Nisbet*, 1973; *Pingree*, 1990]. Recent studies [*Richards*, 1986; *Richards and Khazanov*, 1997], though, have demonstrated that some ambient electrons will gain considerable energy by quenching an excited

[1]Now at Arecibo Observatory, Arecibo, Puerto Rico.

Paper number 1999JA900054.
0148-0227/99/1999JA900054$09.00

state of nitrogen ($N(^2D)$). This quenching adds 2.4 eV to the electron involved.

Computing the energy deposition by energetic electrons created by solar EUV and by the quenching of excited states is a complicated problem owing to the many different collisional events that slow down the energetic electrons and split the available energy between the neutrals, ions, and ambient electron gas [*Cicerone et al.*, 1973]. In addition, at nonequatorial latitudes these energetic electrons can travel long distances along magnetic field lines (even to a conjugate hemisphere) before giving away their energy [*Nisbet*, 1968; *Swartz et al.*, 1975; *Schunk and Nagy*, 1978].

The problem of energetic electron heating and transport generated a lot of interest during the 1960s and 1970s, when much effort was devoted to estimating this effect [e.g., *Nisbet*, 1968; *Nagy and Banks*, 1970; *Swartz and Nisbet*, 1973; *Swartz et al.*, 1975; *Bailey et al.*, 1975; *Swartz*, 1976]. A comprehensive comparison between the most common theoretical methods was performed by *Cicerone et al.* [1973]. These authors found good agreement in the electron heating computed with three different methods, an agreement that was further refined by *Swartz and Stamnes* [1977] and *Swartz* [1985]. Thus, for the purpose of this study, we will use one of the methods considered in the study by *Cicerone et al.* [1973], namely, the method developed by *Nisbet* [1968] and *Swartz and Nisbet* [1973]. This method handles the transport and thermalization of energetic electrons by solving a set of continuity equations (one for each energy interval and altitude) that we simplify here for the local steady state case appropriate to the horizontal magnetic field above Jicamarca and also modify to include the source from quenching of $N(^2D)$

$$n_E(z)v_E\left[\frac{n_e(z)}{\Delta E}L(n_e,E)+\sum_j n(j,z)\sigma_a(j,E)\right]= q_E(z)+q_{\delta(E-2.4-KT_e)}(z). \quad (1)$$

Here $n_E(z)$ is the density of energetic electrons within an energy increment ΔE centered around E at a height z, v_E is the velocity of these fast electrons of energy E, $\sigma_a(j,E)$ is an inelastic collision cross section, n_e is the ambient electron density, $L(n_e,E)$ is the energy loss function to the ambient electron gas given by *Swartz et al.* [1971], $q_E(z)$ is the photoproduction rate of electrons (in units of $cm^{-1}s^{-1}$) within the energy cell centered at energy E, and $q_{\delta(E-2.4-KT_e)}(z)$ is the production rate of electrons with an added energy of 2.4 eV via the quenching of $N(^2D)$. The sum is over all the different neutral species. The photoelectron production rates were estimated from the latest version [*Tobiska and Eparvier*, 1998] of the solar EUV flux model developed by *Tobiska* [1991]. The nitrogen quenching source term is discussed further below.

After solving (1) for $n_E(z)$ using the method of *Swartz* [1985], we sum the contributions from all electron energies to get the total electron heating rate

$$Q_{E,e}(z)\equiv\sum_E v_E L(n_e,E)n_E(z)n_e(z). \quad (2)$$

The quenching electron heat source arises from the reaction

$$N(^2D)+e\xrightarrow{k}N(^4S)+e+2.4\,\mathrm{eV} \quad (3)$$

in which the excited nitrogen atom $N(^2D)$ is brought down to the ground state $N(^4S)$ by a collision with an electron. The rate for this reaction (in cm^3s^{-1}) is given by *Richards* [1986] as

$$k=6.5\times10^{-10}\left(\frac{T_e}{300}\right)^{0.5}. \quad (4)$$

From inspection of (3), we see that in order to estimate the rate at which energy goes into the electrons from this source, it is necessary to know the density of $N(^2D)$. The density of this excited state is not given by the standard neutral atmosphere models nor is it measured directly; nevertheless, it can be estimated under chemical equilibrium by equating the production to the loss.

The reactions producing $N(^2D)$ are summarized in Table 1, with the corresponding production rates given as the products of the basic reaction rates with the $N(^2D)$ production efficiencies as described by *Richards* [1986]. Note that β_2 accounts for the two $N(^2D)$ atoms that can be produced via the dissociative recombination of N_2^+. We plot these rates as a function of altitude in Figure 1 using daytime values of temperature and density at Jicamarca. Figure 1 shows that the reaction with NO^+ dominates over the altitude interval considered in this study, with the dissociative recombination of N_2 becoming a close second in the upper altitudes.

$N(^2D)$ is lost through collisions that bring this excited state down to the ground state or through reactions that interchange atoms with colliding molecules. The operative reactions are given in Table 2. An example of applying these loss rates of $N(^2D)$ to conditions over Jicamarca is shown in Figure 2. The quenching of $N(^2D)$ by electrons exceeds all other losses above $\sim$ 230 km.

By equating the total production of $N(^2D)$ by the reactions shown in Table 1 to the total loss through the reactions in Table 2, one can solve for the equilibrium density of $N(^2D)$; that is,

$$n_{N(^2D)}=\frac{\beta_1 n_{N_2^+}n_O+\beta_2 n_{N_2^+}n_e+\beta_3 n_{NO^+}n_e}{k_1 n_e+k_2 n_O+k_3 n_{O_2}} \quad (5)$$

Table 1. Production of $N(^2D)$

Reaction	Rate, $cm^3\ s^{-1}$
$N_2^+ + O \xrightarrow{\beta_1} NO^+ + N(^2D)$	$\beta_1 = 1.4\times10^{-10}(300/T_n)^{0.44}$
$N_2^+ + e \xrightarrow{\beta_2} 2N(^2D)$	$\beta_2 = 4.2\times10^{-7}(300/T_e)^{0.39}$
$NO^+ + e \xrightarrow{\beta_3} O + N(^2D)$	$\beta_3 = 3.4\times10^{-7}(300/T_e)^{0.85}$

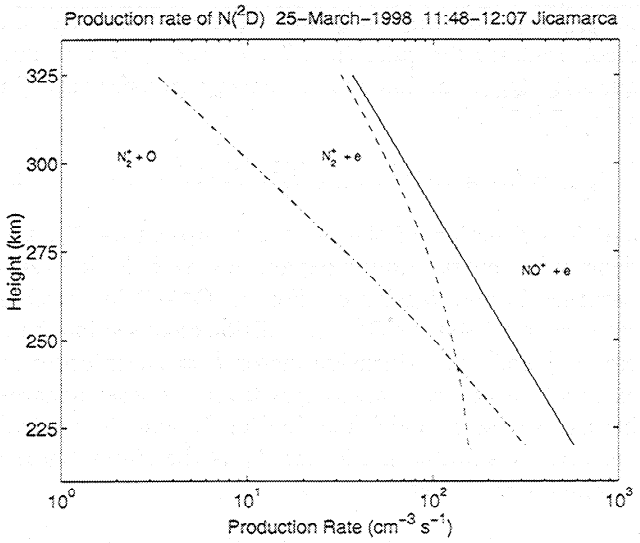

Figure 1. Production rates of $N(^2D)$ from the three sources of Table 1 as a function of height at Jicamarca, March 25, 1998, 1148-1207 LT.

Once the density of $N(^2D)$ is known, the rate at which electrons are energized (in $cm^{-3}s^{-1}$) from this excited state can be computed from

$$\begin{aligned} q_{\delta(E-2.4-KT_e)}(z) &= k_1 n_{N(^2D)} n_e \\ &= 6.5 \times 10^{-10} \left(\frac{T_e}{300}\right)^{0.5} \\ &\quad \times n_{N(^2D)} n_e \end{aligned} \tag{6}$$

where the densities are in cm^{-3} and T_e is in kelvins. The quantity $q_{\delta(E-2.4-KT_e)}(z)$ is the second production term of (1).

Since $N(^2D)$ is produced from NO^+ and N_2^+ (see (5) and Figure 1), we need to estimate the (small) densities of these molecular ions. Measurements from the Atmospheric Explorer show concentrations of NO^+ to be of the order of 10% of the total ionization at 200 km [*Frederick and Rusch*, 1977], and this percentage decreases rapidly at higher altitudes. The density of N_2^+ is less than 1% of the total ion density in the F region. Although we derive various ionospheric parameters in this study from incoherent scatter radar (ISR) data, we cannot directly measure these molecular ion densities. Instead, we estimate the densities from photochemical equilibrium, based on the ion chemistry outlined in Table 3, neutral density models, and the photoproduction of O^+, N_2^+ and O_2^+. Photoproduction of NO^+ from neutral NO in the F region is negligible compared to chemical production [*Bailey and Sellek*, 1990].

The energy $Q_{E,e}$ gained by the ambient electron gas from photoelectrons and deactivation of $N(^2D)$ eventually finds its way to the ions through Coulomb collisions ($Q_{e,i}$) and to the neutrals through elastic and inelastic collisions ($Q_{e,n}$). So we can write

$$Q_{E,e} = Q_{e,i} + Q_{e,n} \tag{7}$$

The various individual cooling rates are given by *Schunk and Nagy* [1978], and we discuss $Q_{e,i}$ further in the next section.

3. Required Parameters and Experimental Analysis

The neutral parameters that go into the calculations of the electron heating and cooling rates are deduced indirectly from incoherent scatter data, the ion energy balance equations, and parameters at a reference height of a model neutral atmosphere. Early estimates of the neutral temperature from ISR data were made by *Nisbet* [1967]. Later *Bauer et al.* [1970] and *Swartz and Nisbet* [1971] showed that neutral atomic oxygen densities could also be determined from ISR data. In our study, we employ the method developed by *Pingree* [1990], in which the fitting of incoherent scatter autocorrelation functions (ACFs) is constrained by the ion energy balance. When this constraint is added, the function that is minimized in the least squares fitting of incoherent scatter ACFs can be written as

$$\begin{aligned} \chi^2 = &\sum_{k=1}^{N_{alt}} \left\{ \sum_{j=1}^{N_{lags}} \frac{[\rho_{kj} - \hat{\rho}(\tau_j, \mathbf{a}_k)]^2}{\sigma_{kj}^2} \right\} \\ &+ \frac{[Q_{e,i}(\mathbf{a}_k) - Q_{i,n}(\mathbf{a}_k)]^2}{\sigma_c^2}. \end{aligned} \tag{8}$$

The term in braces represents the standard height-by-height fitting of model ACFs ($\hat{\rho}(\tau_j, \mathbf{a}_k)$) to the measured ACFs [$\rho_j$], where σ_j^2 is the variance of each data point j (lag of the ACF). The second line contains the constraint function (ion energy balance $Q_{e,i} - Q_{i,n} = 0$) evaluated at the parameter vector $\mathbf{a}_k$. Heights are coupled through the neutral model parameters appearing in the parameter vector (see below). The rate $Q_{e,i}$ is given (in eV $cm^{-3}s^{-1}$) by

Table 2. Loss of $N(^2D)$.

Reaction	Rate, $cm^3\ s^{-1}$	Reference
$N(^2D) + e \xrightarrow{k_1} N(^4S) + e$	$k_1 = 6.5 \times 10^{-10}(T_e/300)^{0.5}$	*Richards* [1986]
$N(^2D) + O \xrightarrow{k_2} N(^4S) + O$	$k_2 = 6.0 \times 10^{-13}$	*Richards et al.* [1981]
$N(^2D) + O_2 \xrightarrow{k_3} NO + O$	$k_3 = 6.0 \times 10^{-12}$	*Richards* [1986]

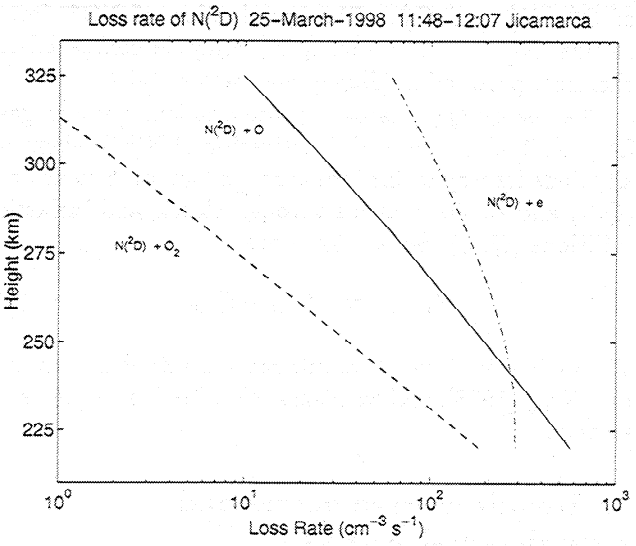

Figure 2. Loss rates of $N(^2D)$ as a function of height at Jicamarca, March 25, 1998, 1148-1207 LT.

$$Q_{e,i} = An_e n_i \frac{T_e - T_i}{T_e^{3/2}} \quad (9)$$

$$A = 3.2 \times 10^{-8} \ln\Gamma$$

where $\ln\Gamma$ is the Coulomb logarithm given by *Itikawa* [1975]

$$\ln\Gamma = \ln\left[\frac{4K_B T_e}{\gamma^2 Ze^2 k_e}\right] - \frac{1}{2}, \quad (10)$$

$\ln\gamma = 0.57722$ is Euler's constant and

$$k_e = \sqrt{\frac{4\pi n_e e^2}{K_B T_e}}, \quad (11)$$

so $Q_{e,i}$ depends only on quantities measurable with an incoherent scatter radar (i.e., T_e, T_i, and $n_e = n_i$). The quantity $Q_{i,n}$, the ion-neutral energy transfer rate (in eV cm^{-3}s^{-1}), is

$$Q_{i,n} = 2.1 \times 10^{-15} n_i n_O \sqrt{T_i + T_n}(T_i - T_n) \quad (12)$$

and is a function of the neutral temperature T_n, the density of neutral atomic oxygen n_O, and the ion temperature T_i and density n_i. For the $O^+ - O$ ion cooling rate we have used the $O^+ - O$ collision cross section from *Banks* [1966] (i.e., Burnside factor $F = 1$). In order to extract the neutral parameters from the least squares fitting, we use a model function for T_n and the neutral density. A suitable model for T_n is the Bates-Walker profile [*Bates*, 1959]

$$T_n(z) = T_\infty - (T_\infty - T_0)e^{-s(z-z_0)}. \quad (13)$$

This model has three parameters: T_∞, T_0, and the shape factor s. We will not fit for these three parameters, however; instead, we will follow the method of *Burnside et al.* [1988] and estimate T_0 and s from the mass spectrometer / incoherent scatter (MSIS) model [*Hedin*, 1987] at 120 km

$$s = \left.\frac{dT_n}{dz}\right|_{z=120} (T_\infty - T_0)^{-1}. \quad (14)$$

The derivative dT_n/dz comes from MSIS temperatures at 119 and 121 km

$$\left.\frac{dT_n}{dz}\right|_{z=120} \approx \frac{T_n(121) - T_n(119)}{2} \quad (15)$$

and T_∞ is one of the parameters of the fit. Furthermore, under diffusive equilibrium and assuming $T_n \approx$ constant

Table 3. F Region Ion Chemistry

Reaction	Rate Coefficient, cm^3 s^{-1}	Reference
$N_2^+ + O \longrightarrow NO^+ + N$	$\gamma_{412} = 1.4 \times 10^{-10}(300/T_i)^{0.44}$	*McFarland et al.* [1974]
$N_2^+ + O \longrightarrow O^+ + N_2$	$\gamma_{212} = 0.07\gamma_{412}(T_i/300)^{0.21}$	*Torr and Torr* [1979]
$N_2^+ + O_2 \longrightarrow O_2^+ + N_2$	$\gamma_{313} = 5 \times 10^{-11}(300/T_i)$	*Lindinger et al.* [1974]
$N_2^+ + O_2 \longrightarrow NO^+ + NO$	$\gamma_{413} = 10^{-14}$	*Swartz and Nisbet* [1973]
$N_2^+ + NO \longrightarrow NO^+ + N_2$	$\gamma_{414} = 3.3 \times 10^{-10}$	*Rees* [1989]
$O^+ + N_2 \longrightarrow NO^+ + N$	$\gamma_{421} = 1.533 \times 10^{-12}$	*St.-Maurice and Torr* [1978]
	$-5.92 \times 10^{-13}(T_f/300)$	$T_f = (7T_i + 4T_n)/11$
	$+8.6 \times 10^{-14}(T_f/300)^2$	
$O^+ + O_2 \longrightarrow O_2^+ + O$	$\gamma_{323} = 3.1 \times 10^{-11}$	*Torr et al.* [1988]
	$-3.7 \times 10^{-14}T_g$	$T_g = (2T_i + T_n)/3$
	$+1.25 \times 10^{-17}T_g^2$	
$O^+ + NO \longrightarrow NO^+ + N$	$\gamma_{424} = 8 \times 10^{-13}$	*Rees* [1989]
$O_2^+ + N_2 \longrightarrow NO^+ + NO$	$\gamma_{431} = 5 \times 10^{-16}$	*Rees* [1989]
$O_2^+ + NO \longrightarrow NO^+ + O_2$	$\gamma_{434} = 4.4 \times 10^{-10}$	*Lindinger et al.* [1975]
$e + N_2^+ \longrightarrow N + N$	$\alpha_1 = 2.2 \times 10^{-7}(300/T_e)^{0.39}$	*Ziph* [1980]
$e + O_2^+ \longrightarrow O + O$	$\alpha_2 = 4 \times 10^{-12}(300/T_e)^{0.7}$	*Torr* [1985]
$e + O^+ \longrightarrow O$	$\alpha_3 = 1.6 \times 10^{-7}(300/T_e)^{0.55}$	*Torr and Torr* [1979]
$e + NO^+ \longrightarrow N + O$	$\alpha_4 = 4.3 \times 10^{-7}(300/T_e)^{0.85}$	*Walls and Dunn* [1974]

in a small height range, the density of atomic oxygen can be approximated by

$$n_O(z) = n_O(z_r)e^{-(z-z_r)/H(z)} \quad (16)$$

with a scale height of

$$H(z) = \frac{K_B T_n(z)}{m_O g(z)} \quad (17)$$

where $n_O(z_r)$ is the density of atomic oxygen at a reference height z_r, g is the gravitational acceleration, and m_O is the mass of atomic oxygen. The value of the density at the reference height $[n_O(z_r)]$ is taken from MSIS at 250 km. The same procedure is used to obtain the density profiles for the other neutral species.

When we fit with the ion energy balance as a constraint (8), we consider all eight heights observed at once, going from $\sim$ 220 km up to $\sim$ 325 km. In this region we have $T_e > T_i$, and the most abundant ion is atomic oxygen. The parameter vector $\mathbf{a}$ in this case contains electron and ion temperatures for the eight heights ($N_{\rm alt} = 8$), an ACF normalization constant for each height, and T_∞; that is,

$$\mathbf{a} = [\ T_e(1) \ \ldots \ T_e(N_{\rm alt}) \ \ T_i(1) \ \ldots \ T_i(N_{\rm alt}) \ \ c(1) \ \ldots \ c(N_{\rm alt}) \ \ T_\infty\ ]^T \quad (18)$$

The electron density at each height is obtained from Faraday rotation in the ISR data.

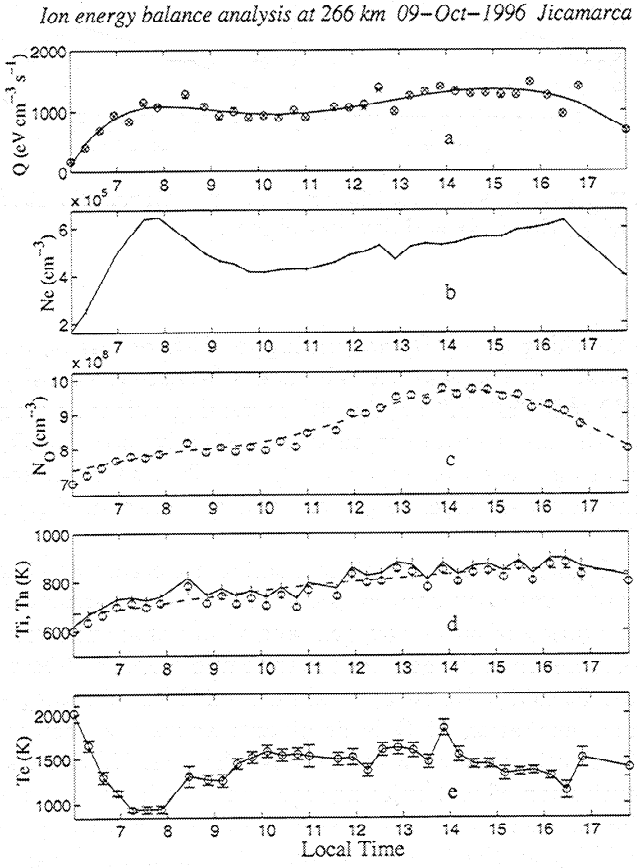

Figure 3. Parameters obtained from incoherent scattering measurements and the ion energy balance at 266 km, October 9, 1996. (a) $Q_{e,i}$ (crosses) and and the nearly identical $Q_{i,n}$ (circles); Solid line is a smoothing curve. (b) Electron density. (c) Atomic oxygen neutral density (circles) and the value given by mass spectrometer/incoherent scatter (MSIS) (dashed line). (d) Ion (solid line) and neutral (circles) temperatures and the value given by MSIS (dashed line). (e) Electron temperature.

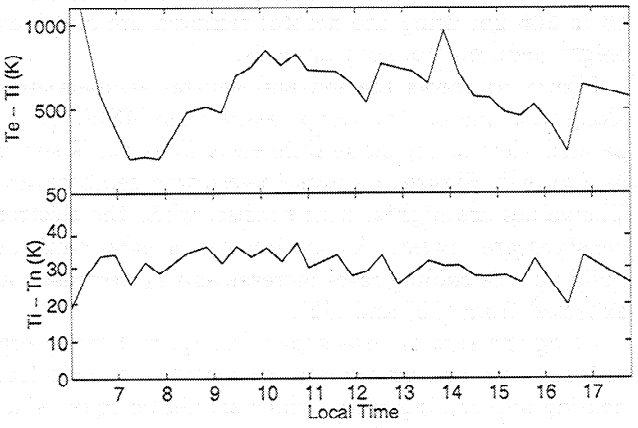

Figure 4. Temperature differences as a function of time at 266 km, October 9, 1996. Note that even though $T_e - T_i$ is very high around sunrise, $T_i - T_n$ is low because n_e is small then and $Q_{e,i} \propto n_e^2$.

4. Results

4.1. Ion Thermal Balance Results

The method just described yields useful results if (1) $T_e - T_i > 0$ and the difference is large enough to be measurable, (2) $T_i - T_n > 0$, and (3) there is only a single ion species (O^+). At Jicamarca these conditions are generally met between 220 and 300-325 km during the day. Figure 3 shows some Jicamarca measurements from 266 km on October 9, 1996, a day of low solar activity. At this height the electron-ion temperature difference is large, and so the much smaller difference $T_i - T_n$ can be estimated reasonably well (see Figure 4). The top panel of Figure 3 shows the diurnal variation of the rate $Q_{e,i}$ at which electrons transfer energy to the ions. The variations in $Q_{e,i}$ in Figure 3 are clearly correlated with variations in electron density (second panel), as expected from (9).

The second quantity displayed in Figure 3a is the rate at which atomic oxygen ions transfer energy to atomic oxygen neutrals ($Q_{i,n}$). We see that for almost all data points $Q_{e,i} \approx Q_{i,n}$, in accordance with the constraint of (8). The solid line in Figure 3a was obtained by fitting a smoothing polynomial to $Q_{e,i}$.

Figure 3b shows the electron density derived from the Faraday rotation data. Figure 3c depicts the density of neutral atomic oxygen, determined by extrapolating the reference height (250 km) value obtained from MSIS-

86 to 266 km using the neutral temperature and scale height deduced from our analysis.

Figure 3d shows the ion and neutral temperatures, along with the neutral temperature from MSIS. An expanded view of the small difference, $T_i - T_n$, is shown in Figure 4. Figure 3e shows the electron temperature. The values are highest near sunrise, when the electron densities are lowest. As the ion and neutral densities build up, the cooling rates increase and T_e decreases, as expected from (10) and (12).

Using the sort of data shown in Figure 3 for several altitudes, we can now compute separately the electron heating and cooling rates (which should be equal, since the electrons are in thermal equilibrium) and compare them, to test our theoretical understanding.

4.2. Electron Energy Balance Results

In this section we examine data from 2 days, one near solar minimum (October 9, 1996; $F_{10.7} \approx 69$) and one with moderate solar activity (March 25, 1998; $F_{10.7} \approx 115$). As we discussed in section 2, we are considering two sources of electron heating: photoelectrons and deactivation of $N(^2D)$. Figure 5 shows the effect of the $N(^2D)$ heating for October 9, 1996. Photoelectron heating is clearly the dominant mechanism, with

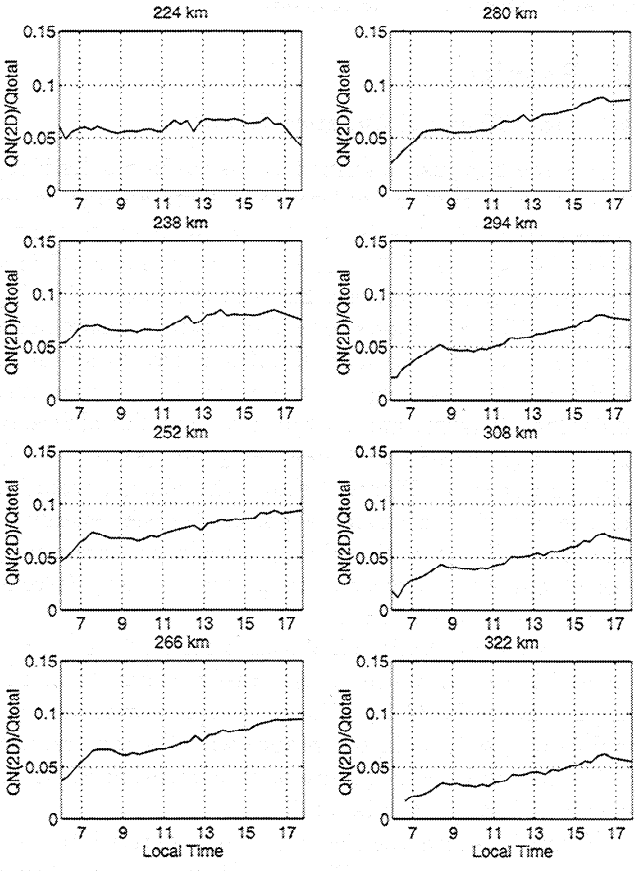

Figure 5. Ratio of $N(^2D)$ heating to total electron heating at Jicamarca on October 9, 1996.

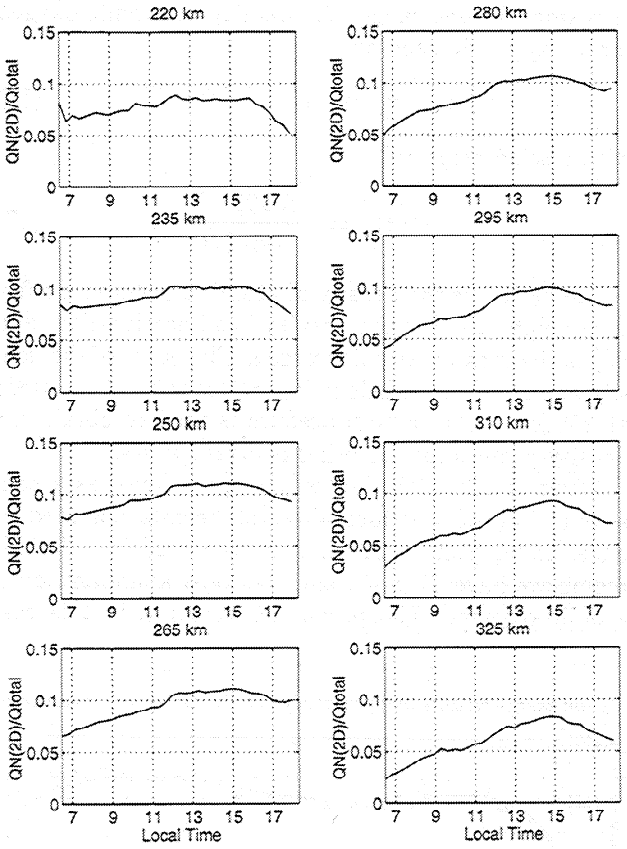

Figure 6. Same as Figure 5, but for March 25, 1998, when the solar activity was higher.

quenching of $N(^2D)$ accounting for 10% or less of the total. The decrease with altitude is because the density of $N(^2D)$ falls off rapidly with increasing altitude owing to the low neutral temperature. Slightly more $N(^2D)$ heating was measured on March 25, 1998, when the solar flux was larger ($F_{10.7} \approx 115$), as shown in Figure 6.

Figure 7 shows the three dominant electron cooling rate terms (Coulomb collisions with ions, fine structure excitation of atomic oxygen, and vibrational excitation of molecular nitrogen) for the solar minimum day (October 9, 1996). Below approximately 250 km, fine structure excitation of O is dominant; above that height, Coulomb collisions with the ions take over. Vibrational excitation of molecular nitrogen remains in third place for all heights, but it is still significant, especially at midday at the lower altitudes. At the upper heights considered in this study (300–322 km) the neutral densities are small and Coulomb collisions dominate the cooling process.

So far, we have restricted our discussion of the cooling rate calculations to the three most dominant mechanisms. There is an assortment of other electron-neutral cooling processes that do not contribute much individually, but their sum can add up to as much as 10–20% of the total cooling at the lower altitudes. These are in-

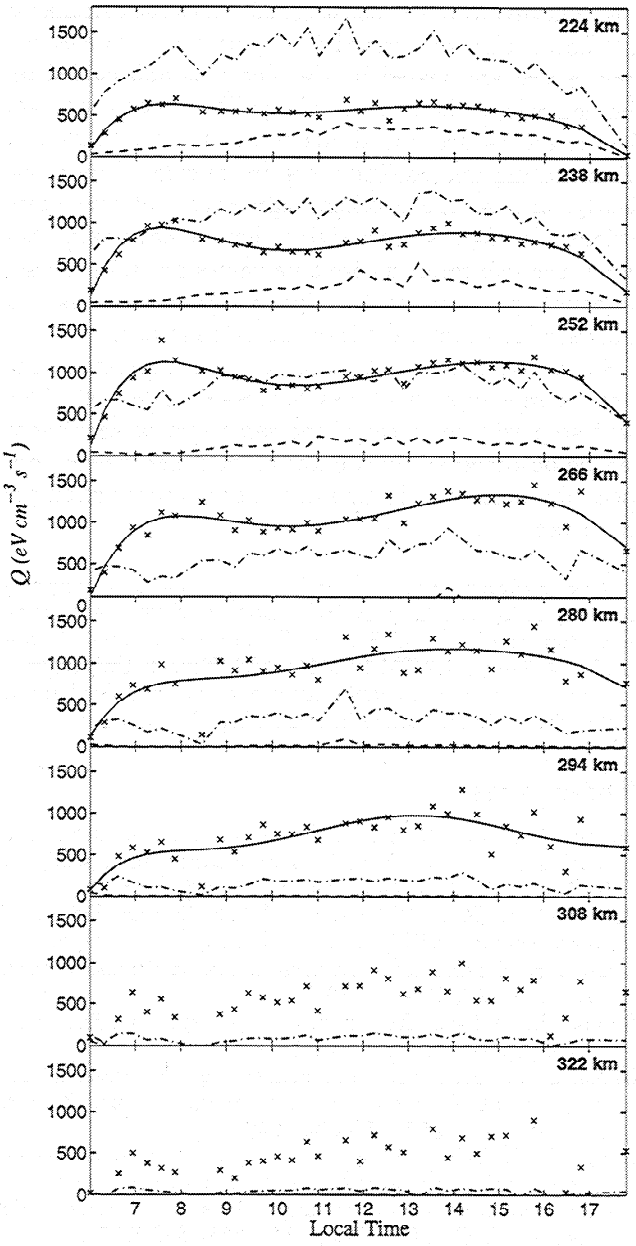

Figure 7. Dominant electron cooling rates between 224 and 322 km at Jicamarca on October 9, 1996, showing fine structure excitation of O (dash-dotted line), vibrational excitation of N_2 (dashed line), coulomb collisions with ions (crosses), and polynomial fit to $Q_{e,i}$ (solid line).

cluded in the calculation of the total cooling rate, which we now compare with the total heating rate. If our models and data are correct, of course, the two values should be equal. Figure 8 shows the solar minimum day comparisons.

The most important point to notice about Figures 8 and 9 is that the heating and cooling rates agree reasonably well. There are differences that seem to depend somewhat on altitude, but these differences are far less than those reported in earlier F region thermal balance studies.

Figure 9 shows the same comparison of the heating and cooling rates for March 25, 1998, the day of moderate solar activity, when the $F_{10.7}$ cm flux was nearly twice the value for the solar minimum day (115 versus 69). We see from Figure 9 that the heating/cooling rates are about twice as large also, but most important is the fact that the agreement between the rates is excellent, even better than for the solar minimum case, except at the upper heights, where the results are obviously noisy, with a large scatter.

5. Summary and Conclusions

In comparing the electron heating and cooling rates at the magnetic equator, we used the most recent mod-

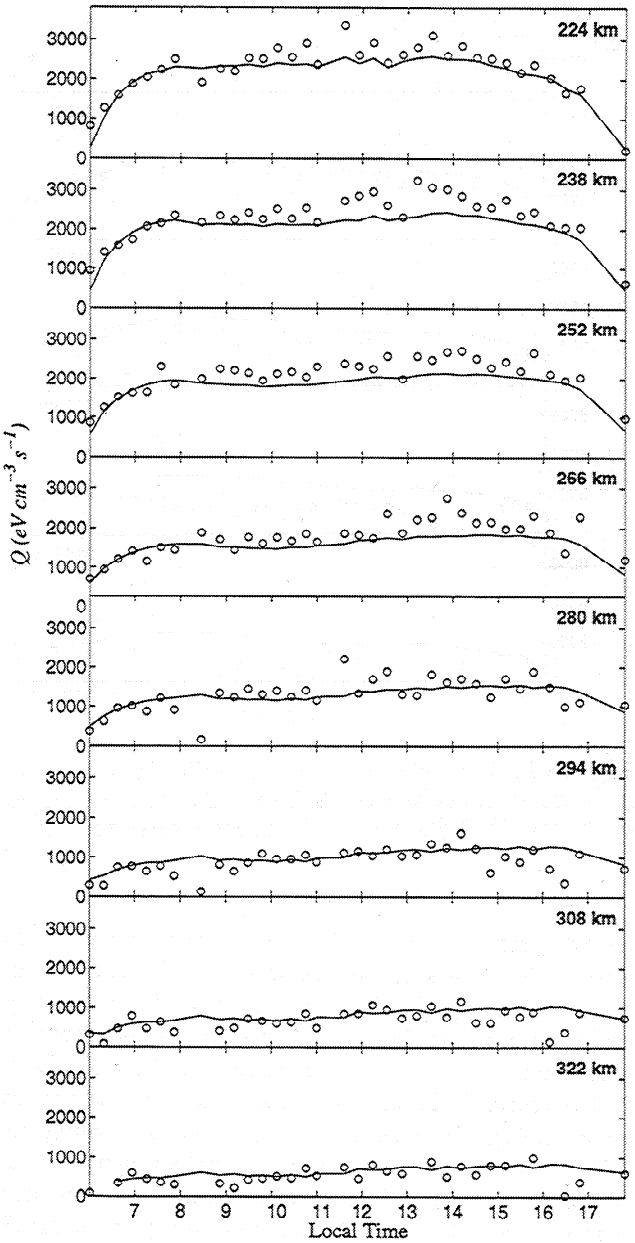

Figure 8. Total electron heating (solid line) and cooling (circles) rates between 224 and 322 km at Jicamarca on October 9, 1996.

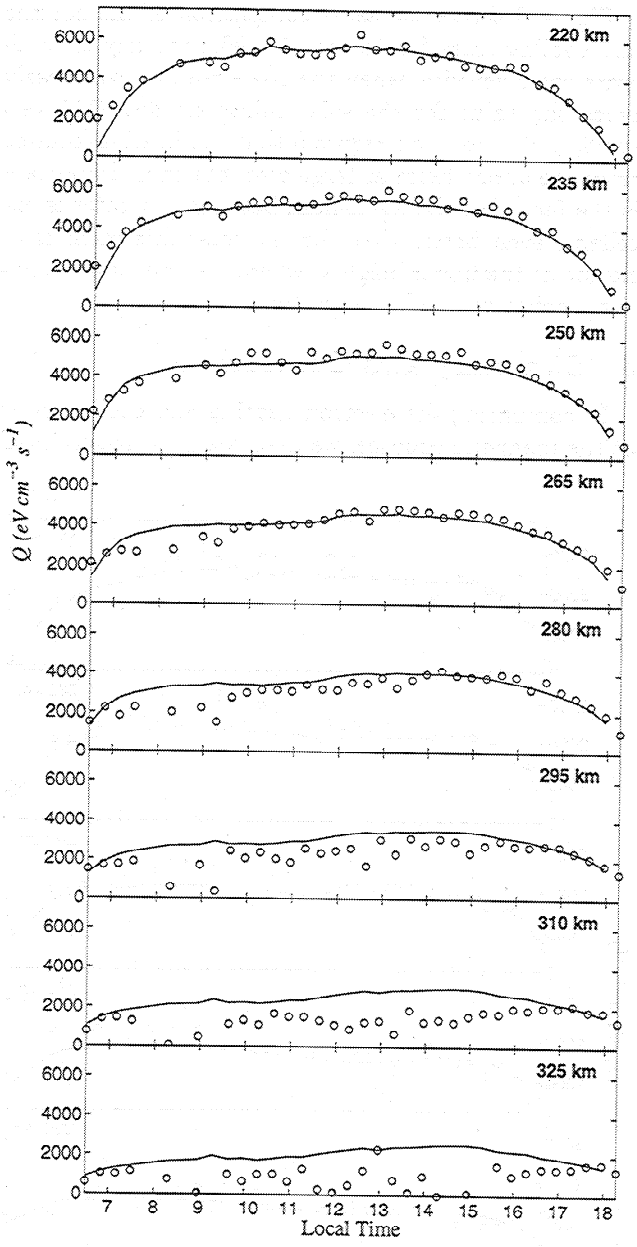

Figure 9. Total electron heating (solid line) and cooling (circles) rates between 220 and 325 km at Jicamarca on March 25, 1998, a day of moderate solar activity.

els and proxies for the EUV flux and the ionization and absorption cross sections. To this we added the heat input provided by the deactivation of $N(^2D)$, which typically amounts to 5–10% of the total. This amount is significant but less than the value of about 30% found in the recent Millstone Hill study [*Richards and Khazanov*, 1997]. To calculate the deactivation cooling, the EUV absorption, and the various electron-neutral cooling rates, we need to know the parameters of the neutral atmosphere. These were deduced partly from MSIS-1986, which provided reference values (T_0 and s) at 120 km for the neutral temperature model and densities at 250 km of the various neutral species. The value of T_∞ was obtained from the constrained fits to the Jicamarca ISR data. The constrained fitting procedure forces the ions, which are heated by the electrons and cooled by the neutrals, to be in thermal equilibrium or nearly so. The electrons are not similarly constrained, however; their heating and cooling rates are calculated independently, and so the excellent agreement, at two quite different levels of solar activity, that we have found between the two rates, whose true values must, of course, be equal, provides strong support for the models and cross sections that went into the calculations.

So we conclude, finally, that we now understand the local energy input and loss processes quite well. The next step will be to see if the same sort of agreement can be obtained at nonequatorial latitudes, where nonlocal photoelectron heating and thermal conduction are important.

Acknowledgments. The Jicamarca Radio Observatory is operated by the Geophysical Institute of Peru with support from the National Science Foundation through Cooperative Agreement ATM-9408441 with Cornell University.

Janet G. Luhmann thanks Knut Stamnes and Graham J. Bailey for their assistance in evaluating this paper.

References

Bailey, G. J., and R. Sellek, A mathematical model of the Earth's plasmasphere and its application in a study of He^+ at L=3, *Ann. Geophys.*, *8*, 171-190, 1990.

Bailey, G. J., R. J. Moffett, and W. E. Swartz, Effects of photoelectron heating and interhemisphere transport on day-time plasma temperatures at low latitudes, *Planet. Space Sci.*, *23*, 599-610, 1975.

Banks, P., Collision frequencies and energy transfer: Ions, *Planet. Space Sci.*, *14*, 1105-1122, 1966.

Bates, D. R., Some problems concerning the terrestrial atmosphere above about the 100 km level, *Proc. R. Soc. London, Ser. A253*, 451-462, 1959.

Bauer, P., P. Waldteufel, and D. Alcayde, Diurnal variations of the atomic oxygen density and temperature determined from incoherent scatter measurements in the ionospheric F region, *J. Geophys. Res.*, *75*, 4825-4832, 1970.

Burnside, R. G., M. P. Sulzer, and J. Walker, Determination of thermospheric temperatures and neutral densities at Arecibo from the ion energy balance, *J. Geophys. Res.*, *93*, 8642-8650, 1988.

Cicerone, R. J., W. E. Swartz, R. S. Stolarski, A. F. Nagy, and J. S. Nisbet, Thermalization and transport of photoelectrons: A comparison of theoretical approaches, *J. Geophys. Res.*, *78*, 6709-6728, 1973.

Frederick, J. E., and D. W. Rusch, On the chemistry of metastable atomic nitrogen in the F region deduced from simultaneous satellite measurements of the 5200 Å airglow and atmospheric composition, *J. Geophys. Res.*, *82*, 3509-3516, 1977.

Hedin, A. E., MSIS-86 thermospheric model, *J. Geophys. Res.*, *92*, 4649-4662, 1987.

Itikawa, Y., Electron-ion energy transfer rate, *J. Atmos. Terr. Phys.*, *37*, 1601-1602, 1975.

Lindinger, W., F. C. Fehsenfeld, A. L. Schmeltekopf, and E. E. Ferguson, Temperature dependence of some ionospheric ion-neutral reactions from 300-900 K, *J. Geophys. Res.*, *79*, 4753-4756, 1974.

Lindinger, W., D. L. Albritton, F. C. Fehsenfeld, and E. E.

Ferguson, Laboratory measurements of the ionospheric $O_2^+(X^2\Pi_g)$ and $O_2^+(a^4\Pi_u)$ reactions with NO, *J. Geophys. Res.*, *80*, 3725-3726, 1975.

McFarland, M., D. L. Albritton, F. C. Fehsenfeld, E. E. Ferguson, and A. L. Schmeltekopf, Energy dependence and branching ratio of the $N_2^+ + O$ reaction, *J. Geophys. Res.*, *79*, 2925-2926, 1974.

Nagy, A. F., and P. M. Banks, Photoelectron fluxes in the ionosphere, *J. Geophys. Res.*, *75*, 6260-6270, 1970.

Nisbet, J. S., Neutral atmospheric temperature from incoherent scatter observations, *J. Atmos. Sci.*, *24*, 586-593, 1967.

Nisbet, J. S., Photoelectron escape from the ionosphere, *J. Atmos. Terr. Phys.*, *30*, 1257-1278, 1968.

Pingree, J. E., Incoherent scatter measurements and inferred energy fluxes in the equatorial F-region ionosphere, Ph.D. thesis, Cornell Univ., Ithaca, N.Y., 1990.

Rees, M. H., *Physics and Chemistry of the Upper Atmosphere*, Cambridge Univ. Press, New York, 1989.

Richards, P. G., Thermal electron quenching of $N(^2D)$: Consequences for the ionospheric photoelectron flux and the thermal electron temperature, *Planet. Space Sci.*, *34*, 689-694, 1986.

Richards, P. G., and G. V. Khazanov, On the thermal electron energy balance in the ionosphere in January 1993 and June 1990, *J. Geophys. Res.*, *102*, 7369–7377, 1997.

Richards, P. G., and D. G. Torr, Ratios of photoelectron to EUV ionization rates for aeronomic studies, *J. Geophys. Res.*, *93*, 4060-4066, 1988.

Richards, P. G., D. G. Torr, and M. R. Torr, Photodissociation of N_2: A significant source of thermospheric atomic nitrogen, *J. Geophys. Res.*, *86*, 1495-1498, 1981.

Richards, P. G., J. A. Fennelly, and D. G. Torr, EUVAC: A solar EUV flux model for aeronomic calculations, *J. Geophys. Res.*, *99*, 8981-8992, 1994.

Schunk, R. W., and A. F. Nagy, Electron temperatures in the F region of the ionosphere: Theory and observations, *Rev. Geophys.*, *16*, 355-399, 1978.

St.-Maurice, J.-P., and D. G. Torr, Nonthermal rate coefficients in the ionosphere: The reactions of O^+ with N_2, O_2, and NO, *J. Geophys. Res.*, *83*, 969-977, 1978.

Swartz, W. E., Thermalization and transport of photoelectrons: A comparison of theoretical approaches, 2, Transport details for isotropic scattering, *J. Geophys. Res.*, *81*, 183-192, 1976.

Swartz, W. E., Optimization of energetic electron energy degradation calculations, *J. Geophys. Res.*, *90*, 6587-6593, 1985.

Swartz, W. E., and J. S. Nisbet, Diurnal variation of the neutral temperature profile at Arecibo from incoherent scatter measurements and its relevance to the 1400-hour density maximum, *J. Geophys. Res.*, *76*, 185-196, 1971.

Swartz, W. E., and J. S. Nisbet, Incompatibility of solar EUV fluxes and incoherent scatter measurements at Arecibo, *J. Geophys. Res.*, *78*, 5640-5657, 1973.

Swartz, W. E., and K. Stamnes, Thermalization and transport of photoelectrons: A comparison of theoretical approaches, 3, Addendum to details for isotropic scattering, *J. Geophys. Res.*, *82*, 2401-2404, 1977.

Swartz, W. E., J. S. Nisbet, and A. E. S. Green, Analytic expression for the energy-transfer rate from photoelectrons to thermal-electrons, *J. Geophys. Res.*, *76*, 8425-8426, 1971.

Swartz, W. E., G. J. Bailey, and R. J. Moffett, Electron heating resulting from interhemispherical transport of photoelectrons, *Planet. Space Sci.*, *23*, 589-598, 1975.

Tobiska, W. K., Revised solar extreme ultraviolet flux model, *J. Atmos. Terr. Phys.*, *53*, 1005-1018, 1991.

Tobiska, W. K., and C. A. Barth, A solar EUV flux model, *J. Geophys. Res.*, *95*, 8243-8251, 1990.

Tobiska, W. K., and F. Eparvier, EUV97: Improvements to EUV irradiance modeling in the soft X-rays and FUV, *Sol. Phys.*, *177*, 147-159, 1998.

Torr, D. G., The photochemistry of the upper atmosphere, in *The Photochemistry of Atmospheres*, edited by J. S. Levine, pp. 165-278, Academic, San Diego, Calif., 1985.

Torr, D. G., and M. R. Torr, Chemistry of the thermosphere and ionosphere, *J. Atmos. Terr. Phys.*, *41*, 797-839, 1979.

Torr, D. G., P. G. Richards, and M. R. Torr, Photochemistry of the ionosphere, in *World Ionosphere Thermosphere Study* WITS *Handbook*, vol 1., edited by C. H. Liu and B. Edwards, pp. 1-38, SCOSTEP Secr., Urbana, Ill., 1988.

Walls, F. G., and G. H. Dunn, Measurement of total cross-sections for electron recombination with NO^+ and O_2^+ using storage techniques, *J. Geophys. Res.*, *79*, 1911-1915, 1974.

Ziph, E. C., The dissociative recombination of vibrationally excited N_2^+ ions, *Geophys. Res. Lett.*, *7*, 645-648, 1980.

N. Aponte, Arecibo Observatory, HC3 Box 53995, Arecibo, PR 00612. (naponte@naic.edu)

D. T. Farley and W. E. Swartz, School of Electrical Engineering, Rhodes Hall, Cornell University, Ithaca, NY 14853. (donf@ee.cornell.edu; wes@ee.cornell.edu)

(Received November, 23, 1998; revised January 28, 1999; accepted January 28, 1999.)